This article has been accepted for publication in a future issue of this journal, but has not been fully edited. Content may change prior to final publication. Citation information: DOI 10.1109/TCBB.2020.2971992, IEEE/ACM Transactions on Computational Biology and Bioinformatics

Using Convolutional Neural Networks to Measure the Physiological Age of *Caenorhabditis elegans*

Jiunn-Liang Lin, Wei-Liang Kuo, Yi-Hao Huang, Tai-Lang Jong, Ao-Lin Hsu and Wen-Hsing Hsu

Abstract—*Caenorhabditis elegans* (*C. elegans*) is a popular and excellent model for studies of aging due to its short lifespan. Methods for precisely measuring the physiological age of *C. elegans* are critically needed, especially for antiaging drug screening and genetic screening studies. The effects of various antiaging interventions on the rate of aging in the early stage of the aging process can be determined based on the quantification of physiological age. However, in general, the age of *C. elegans* is evaluated via human visual inspection of morphological changes based on personal experience and subjective judgment. For example, the rate of motor activity decay has been used to predict lifespan in early- to mid-stage aging. Using image processing, the physiological age of *C. elegans* can be measured and then classified into periods or classes from childhood to elderhood (e.g., 3 periods comprising days 0–2, 4–6 and 10–12) by using texture entropy (Shamir, L. et al., 2009). Our dataset consists of 913 microscopic images of *C. elegans*, with approximately 60 images per day from day 1 to day 14 of adulthood. We present quantitative methods to measure the physiological age of *C. elegans* with convolution neural networks (CNNs), which can measure age with a granularity of days rather than periods. The methods achieved a mean absolute error (MAE) of less than 1 day for the measured age of *C. elegans*. In our experiments, we found that after training and testing our dataset, 5 popular CNN models, 50-layer residual network (ResNet50), InceptionV3, InceptionResNetV2, 16-layer Visual Geometry Group network (VGG16) and MobileNet, measured the physiological age of *C. elegans* with an average testing MAE of 1.58 days. Furthermore, based on the results, we propose two models, one model for linear regression analysis and the other model for logistic regression, that combine a CNN model and a new attribute: curved_or_straight. The linear regression analysis model achieved a test MAE of 0.94 days; the logistic regression model achieved an accuracy of 84.78% with an error tolerance of 1 day.

Index Terms—*Caenorhabditis elegans*, *C. elegans*, Convolution neural networks, CNN, Aging

1 Introduction

AGING is a highly complex and multifactorial biological process [1]. Over the years, *Caenorhabditis elegans* (*C. elegans*) has become a very popular and important model for aging research, mainly due to its short lifespan [2]. A population of *C. elegans*, maintained throughout life at 25 ^{o}C, has a mean lifespan of 12.1 days with a standard deviation of 2.3 days from hatching [3]. Determining how to measure the physiological age of *C. elegans* is fundamental and important work. The physiological characteristics of movement wave frequency, defecation frequency and whole-body water efflux have been studied as functions of age [4]. The rate of motor activity decline may potentially be treated as an indicator of healthspan [5]. Similarly, maximum movement velocity, if measured in mid-adulthood, could be predictive of maximal lifespan [6]. Using the decline in the population mean defecation frequency, the physiological age of *C. elegans* can be differentiated into three periods: days 3-6, days 6-9 and days 9-14. Additionally, age-related changes in *C. elegans* have been identified, including neuromuscular behavioral changes, reproductive changes, morphological changes, and biochemical changes [7]. Traditionally, such age-related changes have been measured by using a dissecting microscope or biochemical assays. Z. Feng et al. listed 144 specific phenotypic parameters, including 59 distinct features, and quantified *C. elegans* behavioral patterns by recording the behaviors of individual nematodes over long time periods. To automate the measurements of specific features (age-related changes), image processing technology was introduced. For example, a tracking and imaging system for the automatic analysis of morphology and behavior in *C. elegans* was proposed in 2004 [8]. C. Restif et al. presented a training-based method that can automatically and simultaneously track and segment multiple swimming worms [9]. J. Johnston et al. used pattern recognition to quantitatively track tissue architecture during adulthood and aging in the *C. elegans* pharynx and to identify the discrete stepwise transitions between distinct morphologies with age-

- *Jiunn-Liang Lin is with the Department of Electrical Engineering, National Tsing Hua University in Hsinchu, Taiwan, and the Information and Communications Research Laboratories, Industrial Technology Research Institute in Chutung, Hsinchu, Taiwan. E-mail: allan.lin@itri.org.tw*
- *Wei-Liang Kuo is with the Department of Electrical Engineering, National Tsing Hua University in Hsinchu, Taiwan. E-mail: doron5322083@yahoo.com.tw*
- *Yi-Hao Huang and Ao-Lin Hsu are with the Institute of Biochemistry and Molecular Biology, National Yang-Ming University in Taipei, Taiwan. Ao-Lin Hsu is the corresponding author for biology. E-mail: {yihaohuang, alhsu}@ym.edu.tw;*
- *Tai-Lang Jong and Wen-Hsing Hsu are with the Department of Electrical Engineering, National Tsing Hua University in Hsinchu, Taiwan. Tai-Lang Jong is the corresponding author for neural networks. E-mail: {tljong, whhsu}@mx.nthu.edu.tw*

1545-5963 (c) 2019 IEEE. Personal use is permitted, but republication/redistribution requires IEEE permission. See http://www.ieee.org/publications_standards/publications/rights/index.html for more information.
xxxx-xxxx/0x/$xx.00 © 2020 IEEE Published by the IEEE Computer Society
Authorized licensed use limited to: University of Exeter. Downloaded on May 03,2020 at 19:53:28 UTC from IEEE Xplore. Restrictions apply.

This article has been accepted for publication in a future issue of this journal, but has not been fully edited. Content may change prior to final publication. Citation information: DOI 10.1109/TCBB.2020.2971992, IEEE/ACM Transactions on Computational Biology and Bioinformatics

grouped pharynx images [10]. However, these automated methods for measuring the age of *C. elegans* can differentiate *C. elegans* into only certain periods or groups from childhood to elderhood, which are not precise and quantitative enough for modern aging studies.

Recently, the technology of deep learning neural networks has been rapidly developing. Convolutional neural networks (CNNs) [11] are a kind of deep learning neural network that have been broadly applied to many domains, including object tracking, pose estimation, text detection and recognition, visual saliency detection, action recognition, and scene labeling. Many CNN models have been developed and have shown high performance in image processing [12]. The ImageNet Large Scale Visual Recognition Challenge (ILSVRC) evaluates these algorithms in object detection and image classification with a large-scale training data containing 1.2 million images and validation and test data containing 150,000 photographs. The dataset has remained unchanged since ILSVRC 2012 [13]. Classification errors decreased from 0.28% in 2012 to 0.023% in 2017 [14]. Many issues in the domain of computer vision have been re-examined from the perspective of this new method [15]. In addition, deep learning has been introduced in many bioinformatics applications, such as sequence analysis, structure prediction and reconstruction, biomolecular property and function prediction, biomedical image processing and diagnosis, and biomolecule interaction prediction and systems biology [16]. For examples, R. Umarov et al. developed a deep learning approach and successfully discriminated short promoter and non-promoter sequences [17]. Y. Li et al. used a CNN component to extract convolutional features and an RNN component to extract sequential features from individual inputs of sequence-length-dependent raw feature encoding [18]. Recently, Z. Xia et al. proposed a poly(A) signal motif agnostic deep learning model for PAS recognition with high accuracy [19]. Furthermore, CNNs have been introduced in biomedical studies [20] for applications such as protein-DNA binding prediction [21] and miRNA target prediction [22].

In this paper, we exploit the image recognition capabilities of CNNs to accomplish the precise and quantitative measurement of physiological age in *C. elegans* with microscopic images of *C. elegans*. We propose 2 CNN models, one for linear regression analysis to determine a continuous value of age and one for logistic regression to classify and find the discrete value of age. The rest of this paper is organized as follows. Related work is summarized in Section 2. The materials and proposed models are described in Section 3. Section 4 presents the experimental results. Finally, the discussion and conclusion are presented in Section 5.

2 Related Work

2.1 Related work on the quantitative measurement of aging

To automatically measure aging in *C. elegans*, many studies have introduced image processing technologies. C Restif and D. Metaxas presented a method for automatically tracking and segmenting the swimming motion of *C. elegans* [9]. Based on swimming pattern, the vigor of *C. elegans* could be measured and analyzed quantitatively, which represented the neuromuscular functional aging of *C. elegans*. C. Huang et al. measured the declines in pharyngeal pumping, body movement, and self-progeny production of *daf-2, age-1, daf-16, eat-2*, and *clk-1* mutants and defined three states of pharyngeal pumping: fast (>149 contractions per minute), slow (6–149 contractions per minute), and nonsignificant (<6 contractions per minute) [23]. Regarding body movement, nematodes were classified into 2 classes: fast moving, in which movements are continuous and sinusoidal, and not fast-moving, in which movements are discontinuous or sluggish. Using these measurements, a staging system was created to describe the aging process. However, C. Huang et al.'s study [23] mainly focused on neuromuscular functional aging. J. Johnston et al. used differential interference contrast microscopy to image the terminal bulb region and presented a computational pharynx model that converted each image into a point (age-defined class) in a weighted feature space [10]. J.-L. Lin et al. focused on preprocessing microscopic images of *C. elegans* to automatically segment out *C. elegans* to facilitate aging measurements [24]. Using this segmentation approach, L. Shamir et al. were able to measure the image texture entropy of the pharynx terminal bulb of *C. elegans* and classify the age of *C. elegans* into 3 periods: days 0–2, days 4–6 and days 10–12 [25].

2.2 Related work on CNN models

Since 2012, many CNN models have been used in ILSVRC, and their advantages for image recognition have been described. In this study, we selected a 50-layer residual network (ResNet50), InceptionV3, InceptionResNetV2, a 16-layer Visual Geometry Group network (VGG16), and MobileNet as candidate CNN models. These models are all successful types of CNN models and are benchmarks in ILSVRC [26].

ResNet50 [27]

The more layers a neural network has, the more difficult it is to train. Moreover, deeper networks have greater numbers of training and test errors (Fig. 1 in [27]). However, owing to the residual functions, which might generally be closer to zero than the non-residual functions, ResNet reformulates the layers as learning residual functions with respect to the layer inputs instead of learning an unreferenced function, which facilitates optimization. ResNet with 34 parameter layers was the winner of ILSVRC 2015, with a top-5 error rate of 3.57%. The more layers that ResNet has, the faster responses are generated. ResNet50 is a version of ResNet with 50 layers, with each 2-layer block in the 34-layer network being replaced with a 3-layer bottleneck block.

InceptionV3 and InceptionResNetV2 [28-31]

The Inception networks were proposed by C. Szegedy et al. at Computer Vision and Pattern Recognition (CVPR) 2015, and they were the winners of ILSVRC 2014 in the classification track, with a top-5 error rate of 6.67% (Table 2 in

1545-5963 (c) 2019 IEEE. Personal use is permitted, but republication/redistribution requires IEEE permission. See http://www.ieee.org/publications_standards/publications/rights/index.html for more information.
Authorized licensed use limited to: University of Exeter. Downloaded on May 03,2020 at 19:53:28 UTC from IEEE Xplore. Restrictions apply.

This article has been accepted for publication in a future issue of this journal, but has not been fully edited. Content may change prior to final publication. Citation information: DOI 10.1109/TCBB.2020.2971992, IEEE/ACM Transactions on Computational Biology and Bioinformatics

[28]). Inception networks mainly enhance the processing utilization and optimization of deep CNNs. Subsequent versions of the Inception network were created with improved performance, such as InceptionV2, InceptionV3 and InceptionV4. InceptionV2 normalizes each training mini-batch and achieves the same accuracy with 14 times fewer training steps than Inception. InceptionV3 scales up the network to utilize the computation by suitably factorized convolutions and aggressive regularization and achieved top-1 and top-5 error rates of 21.2% and 5.6%, respectively, in single-frame evaluation in the ILSVRC 2012 classification task. InceptionV4 has a more uniform, simplified architecture and more Inception modules than InceptionV3. InceptionV4 achieved top-1 and top-5 error rates of 17.7% and 3.8%, respectively. InceptionResNetV2 is a residual version of the Inception networks and achieves a greater improvement in recognition performance than the "pure" Inception networks (Table 1 and Table 2 in [31]).

VGG16 [32]

Simonyan and Zisserman proposed the VGG networks, which have small (3x3) convolution filters, and attained first and second place in the localization and classification tracks at ILSVRC 2014, respectively. VGG evaluated networks of increasing depth (16-19 layers) and showed that the representation depth improved the classification accuracy. At the 2014 ILSVRC, VGG achieved top-1 and top-5 error rates of 24.7% and 7.5%, respectively. VGG was the winner of the localization track at ILSVRC 2014, with 25.3% error. VGG16 is the 16-layer version of VGG.

MobileNets [33]

MobileNets are efficient models for mobile and embedded vision applications, adopting a depth-wise separable convolution, two hyper-parameters, a width multiplier and a resolution multiplier to build small, low-latency models to satisfy application requirements. The depth-wise separable convolution factorizes a standard convolution into a depthwise convolution and a pointwise convolution, and it has a computational cost between 8 to 9 times less than that of the standard convolution, with a small reduction in accuracy. Hyperparameters were used for the construction of a smaller neural network with lower computational cost. MobileNet showed an accuracy of 70.6% on ImageNet, which is similar to that of VGG16 and GoogleNet. However, MobileNet is 32.86 times smaller and requires 26.89 times less computation than VGG16. Additionally, MobileNet is 1.62 times smaller and requires 2.72 times less computational cost than GoogleNet (Table 8 in [33]).

3 Material and Methods

3.1 Material

Wild-type (N2) *C. elegans* was cultured at 20 °C on nematode growth medium (NGM) plates. The eggs were collected and were allowed to develop into 1-day-old young adults. One-day-old adult worms were placed on each OP50 bacteria-seeded plate. The worms were then transferred to new plates with fresh bacteria every 2 days until reproduction ceased. Before recording the images, the worms were placed on an agar pad and anesthetized with 25 mM sodium azide (NaN3). Images of at least 30 worms were taken at each time point. Bright-field microscopic images of worms were photographed by an OLYMPUS microscope (BX63) and du-al-chip camera (DP80) under standard 10X eyepieces (OLYMPUS WHN10X/22) and 10X objectives (OLYM-PUS UPLFLN10X2), with a 10 mm working distance and 0.3 numerical apertures. All images were focused on the alimentary system of the worms. The exposure time was set to 50 μs. The graphic resolution was set to 1360 x 1024 pixels. The original image files were all converted to JPEG images for analysis. Representative microscopic images are shown in Fig. 1. We obtained 913 microscopic images of *C. elegans,* representing approximately 60 nematodes per day, and labeled each image by age from day 1 to day 14.

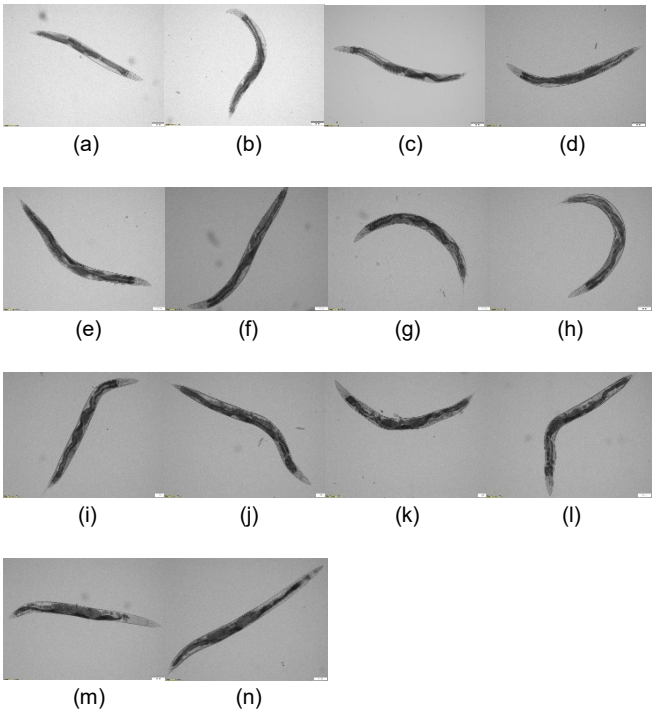

Fig. 1 Microscopic images of *C. elegans* at (a) day 1, (b) day 2, (c) day 3, (d) day 4, (e) day 5, (f) day 6, (g) day 7, (h) day 8, (i) day 9, (j) day 10, (k) day 11, (l) day 12, (m) day 13, and (n) day 14 of adulthood.

3.2 Methods

Our experiment had two stages. In the first stage, we implemented the testing architecture shown in Fig. 2 for 5 models, VGG16, InceptionV3, InceptionResNetV2, MobileNet and ResNet50, in sequence, to find the best-performing CNN models among them. The proposed testing model adopted a global average pooling layer [34] to connect the last layers with the CNN model and one cell as the output layer to determine the age of *C. elegans*. Each CNN model was fitted sequentially into the testing model. During the training process, the testing model was trained with the image dataset described in Section 3.1; 70% of the images were randomly selected for training the model, and 20% of the images were randomly selected for validating

1545-5963 (c) 2019 IEEE. Personal use is permitted, but republication/redistribution requires IEEE permission. See http://www.ieee.org/publications_standards/publications/rights/index.html for more information.
Authorized licensed use limited to: University of Exeter. Downloaded on May 03,2020 at 19:53:28 UTC from IEEE Xplore. Restrictions apply.

This article has been accepted for publication in a future issue of this journal, but has not been fully edited. Content may change prior to final publication. Citation information: DOI 10.1109/TCBB.2020.2971992, IEEE/ACM Transactions on Computational Biology and Bioinformatics

the model. The loss function was the mean square error, and the errors of validation and test were the mean absolute error (MAE). After the training process finished, the trained CNN model was tested with the remaining 10% of the images in the dataset.

TABLE 1
THE MEASUREMENT OF *C. ELEGANS* AGE USING THE TESTING NETWORK SHOWN IN FIG. 2 WITH DIFFERENT TYPES OF CNN MODELS: RESNET50, INCEPTIONV3, INCEPTIONRESNETV2, VGG16 AND MOBILENET

	Validation		Test
	Loss (day^2)	MAE (days)	MAE (days)
ResNet50	4.08	1.55	1.80
InceptionV3	2.28	1.18	1.25
InceptionResNetV2	2.04	1.05	1.18
VGG16	7.27	2.19	2.38
MobileNet	2.01	1.06	1.28

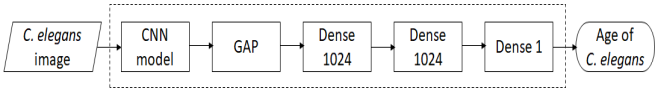

Fig. 2 The testing neural network model in the dashed rectangle is designed to measure the age of *C. elegans* and uses a pure CNN model. The testing neural network model produces a continuous value of age from the inputted *C. elegans* image.

Employing the testing architecture in the first stage, the models presented great capabilities in measuring *C. elegans* age, as shown in Table 1. The quantitative measurement of *C. elegans* age achieved an average MAE of 1.58 days.

As shown in Table 1, ResNet50 achieved an MAE of 1.55 days in the validation part of the training process and an MAE of 1.80 days during the testing phases with untrained images. InceptionV3 and InceptionResNetV2 outperformed ResNet50; their MAEs in the validation phase of the training process were 1.18 days and 1.05 days, respectively. Moreover, the MAEs of InceptionV3 and InceptionResNetV2 in the testing phase with untrained images were 1.25 days and 1.18 days, respectively, as shown in Table 1. However, when using VGG16, the validation MAE in the training process was higher, 2.19 days, and the MAE while testing with untrained images was 2.38 days (Table 1). Using MobileNet for the testing model shown in Fig. 2 and working with the same image dataset, we achieved an MAE of 1.06 days in the validation phase and an MAE of 1.28 days in the testing phase with untrained images.

In the second stage, we introduced an additional attribute to cooperate with the CNN models. The human visual system considers both the local features (e.g., texture) and global features (e.g., contour) of an object for recognition. However, CNNs mainly rely on local features, such as feature points and angles, and some important global structured features, such as contour, are lost [35]. Because of the lack of data on age-related changes in *C. elegans*, we chose an additional attribute (curved_or_straight) as a global feature and cooperated with the top 2 CNN models, separately, in terms of performance in Table 1 to conduct a performance test. With curved_or_straight, we expected to reduce the number of incorrect matches of straight *C. elegans* and curvy *C. elegans* and to improve the recognition performance of CNN models. The performance test in the second stage contained two parts: one for regression analysis [36] and one for logistic regression [37]. We proposed two models that contained the selected CNN model, as shown in Fig. 3 and Fig. 4, respectively.

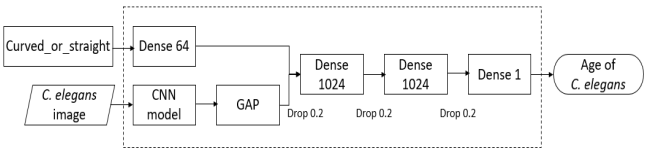

Fig. 3 The proposed model, enclosed in the dashed rectangle, is designed for regression analysis. The inputs of the proposed model are a *C. elegans* image and the attribute curved_or_straight, and the output is a continuous value of age.

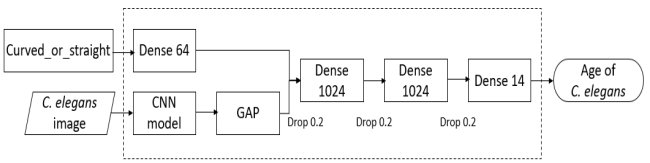

Fig. 4 The proposed model, enclosed in the dashed rectangle, is designed for logistic regression. The inputs of the proposed model are a *C. elegans* image and the attribute curved_or_straight, and the output is a discrete value of age.

The proposed model enclosed in the dashed rectangle in Fig. 3, which introduces global average pooling and a dense layer for curved_or_straight, was designed for regression analysis and directly outputs a continuous value of physiological age of *C. elegans*. The attribute curved_or_straight is manually assigned according to the shape of *C. elegans* in the microscopic picture. The second proposed model, which is enclosed in the dashed rectangle in Fig. 4, was designed for logistic regression and differentiated all *C. elegans* nematodes into 14 classes to determine a discrete physiological age value for *C. elegans*. Each class represents the specific age from day 1 to day 14. The difference between these two models, shown in Fig. 3 and Fig. 4, is that the last dense layer in Fig. 4 has 14 cells instead of 1 cell. In the implementation, the loss function adopts the mean square error function in Fig. 3 and adopts the cross-entropy function in Fig. 4. Regarding the activation function, rectified linear unit (ReLU) is used for all layers in Fig. 3 and Fig. 4 except for the output layer in Fig. 4, which is replaced by the softmax function.

1545-5963 (c) 2019 IEEE. Personal use is permitted, but republication/redistribution requires IEEE permission. See http://www.ieee.org/publications_standards/publications/rights/index.html for more information.
Authorized licensed use limited to: University of Exeter. Downloaded on May 03,2020 at 19:53:28 UTC from IEEE Xplore. Restrictions apply.

This article has been accepted for publication in a future issue of this journal, but has not been fully edited. Content may change prior to final publication. Citation information: DOI 10.1109/TCBB.2020.2971992, IEEE/ACM Transactions on Computational Biology and Bioinformatics

4 Results

In the image dataset of *C. elegans*, we found some nematodes that had greater curvature than others, as shown in Fig. 5. Therefore, we tried to classify the images of *C. elegans* into two groups: curvy nematodes and straight nematodes. Then, we chose the top 2 CNN models in terms of performance in Table 1, InceptionV3 and InceptionResNetV2, and repeated the same testing process as in the first stage with the testing architecture shown in Fig. 3: 70% of the images were randomly selected for training the model, 20% of the images were randomly selected for validating the model, and the remaining 10% of the images were used for the last test after training. With the 32 neurons for the curved_or_straight attribute, we obtained the results shown in Table 2.

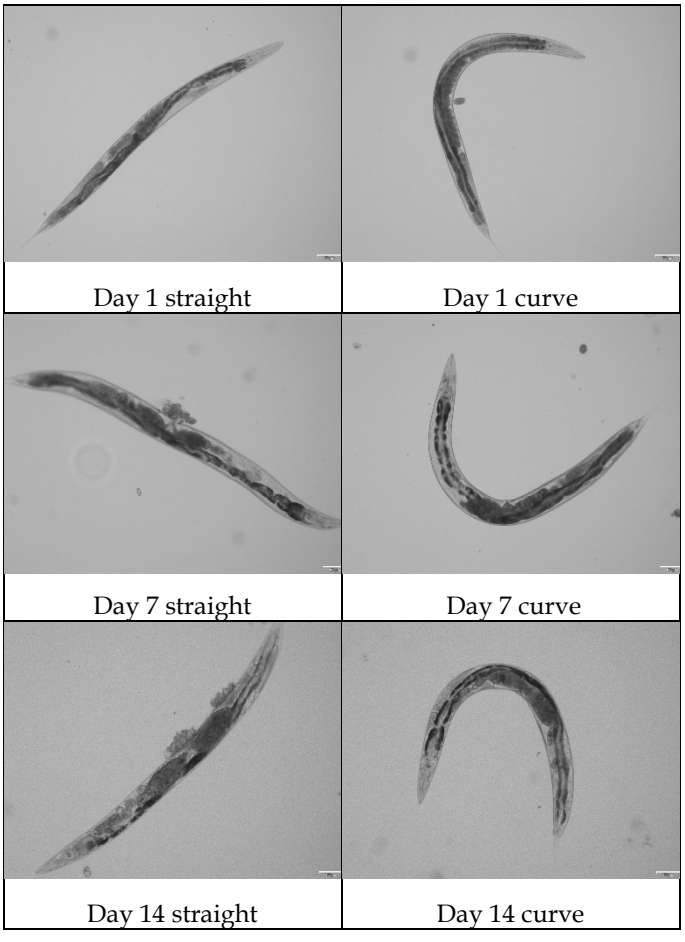

Fig. 5 Microscopic images of *C. elegans* nematodes with straight or curvy shapes.

After implementing the testing architecture shown in Fig. 3 with InceptionV3, the MAEs of the validation and testing phases increased from 1.18 days to 1.23 days and from 1.25 days to 1.51 days, respectively. However, when implementing the testing architecture shown in Fig. 3 with InceptionResNetV2, the MAEs of the validation and testing phase decreased from 1.05 days to 1.01 days and from 1.18 days to 0.96 days, respectively. The MAE for the testing phase was thus, in some cases, less than 1 day when the proposed model shown in Fig. 3 was used with InceptionResNetV2. For further tests, the testing process was repeated using the testing architecture shown in Fig. 3 with InceptionResNetV2 while changing the number of cells in the first dense layer of the proposed model shown in Fig. 3 for the curved_or_straight neurons to 16, 64, 96, and 128 in turn. The results are shown in Table 3.

TABLE 2
THE MEASUREMENT OF *C. ELEGANS* AGE USING THE TESTING ARCHITECTURE SHOWN IN FIG. 3 WITH INCEPTIONV3 AND INCEPTIONRESNETV2, SEPARATELY. THE FIRST DENSE LAYER OF THE PROPOSED MODEL SHOWN IN FIG. 3 CONTAINS 32 CELLS FOR CURVED_OR_STRAIGHT

(with curved_or_straight_32)	Validation of the trained model		Test
	Loss (day^2)	MAE (days)	MAE (days)
InceptionV3	2.36	1.23	1.51
InceptionResNetV2	1.74	1.01	0.96

TABLE 3
THE MEASUREMENT OF *C. ELEGANS* AGE USING THE TESTING ARCHITECTURE SHOWN IN FIG. 3 WITH INCEPTIONRESNETV2 AND DIFFERENT CURVED_OR_STRAIGHT CELLS AT THE FIRST DENSE LAYER OF THE PROPOSED MODEL SHOWN IN FIG. 3

Number of cells for curved_or_straight	Validation		Test
	Loss (day^2)	MAE (days)	MAE (days)
16	2.20	1.11	1.28
32	1.74	1.01	0.96
64	1.48	0.91	0.94
96	1.77	1.01	0.96
128	1.78	1.00	1.03

As shown in Table 3, if 16 neurons were used for the curved_or_straight attribute, the validation and test MAEs were 1.11 days and 1.28 days, respectively. However, if 128 neurons were used for the curved_or_straight attribute, the validation and test MAEs were 1.00 days and 1.03 days, respectively. Although the validation and test MAEs were much smaller when using 128 cells than when using 16 cells at the first dense layer of the proposed model for curved_or_straight, the use of 128 cells was not the best case in the performance test. In Table 3, we found that the test case with 64 cells had the best performance, with an MAE of 0.94 days for the measurement of *C. elegans* age. The test case with 64 neurons seems to be the point at the bottom of the concave curve of performance. When distributing all the measurements of *C. elegans* age on the map of age prediction (Fig. 6), we found that the accuracy of the age prediction reached 55.46%, with an error tolerance of 1 day. If the error tolerance was increased to 2 days, the accuracy of the prediction increased to 88.92%. The results of the experiment provide important information for aging

1545-5963 (c) 2019 IEEE. Personal use is permitted, but republication/redistribution requires IEEE permission. See http://www.ieee.org/publications_standards/publications/rights/index.html for more information.
Authorized licensed use limited to: University of Exeter. Downloaded on May 03,2020 at 19:53:28 UTC from IEEE Xplore. Restrictions apply.

This article has been accepted for publication in a future issue of this journal, but has not been fully edited. Content may change prior to final publication. Citation information: DOI 10.1109/TCBB.2020.2971992, IEEE/ACM Transactions on Computational Biology and Bioinformatics

studies. The proposed model shown in Fig. 3 accomplishes precise and quantitative measurement of the physiological age of *C. elegans*, which is valuable for studies of aging.

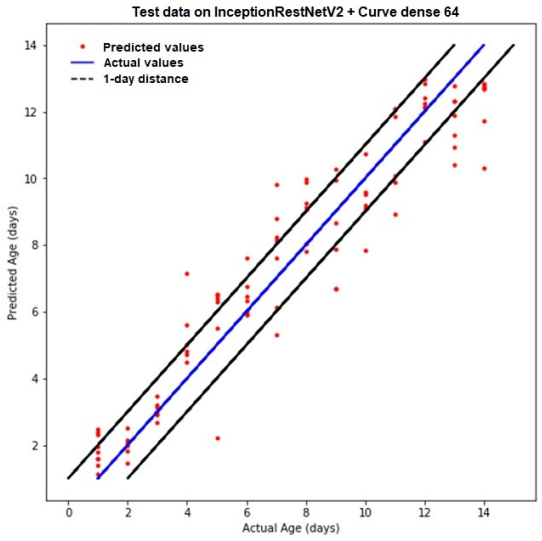

Fig. 6 The distribution of the measured physiological ages of *C. elegans* after completing the testing process with the testing architecture, which consists of InceptionResNetV2 and 64 cells in the first dense layer of the proposed model for curved_or_straight, as shown in Fig. 3. The central line is the real age of the *C. elegans* in the final test. The two outer lines are the lines with the 1-day distance corresponding to the linear regression line.

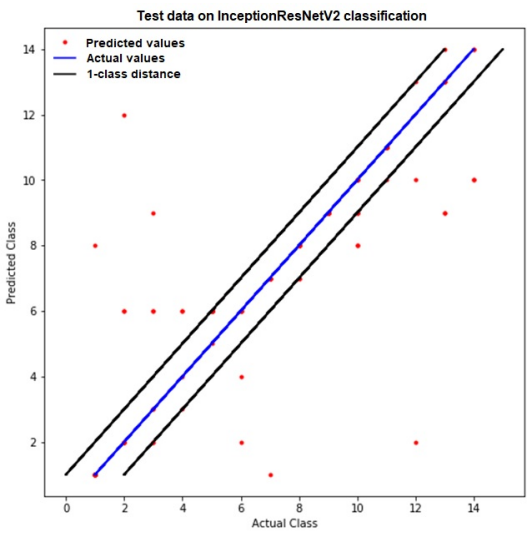

Fig. 7 The distribution of the measured physiological ages of C. elegans after completing the testing process using the testing architecture, which consists of InceptionResNetV2 and 64 cells for at the first dense layer of the proposed model for curved_or_straight, which is shown in Fig. 4. The central line is the real age/class of C. elegans in the final test. The two outer lines are the lines with a 1-class distance corresponding to the blue line.

The last test employed the testing architecture shown in Fig. 4. The proposed model, represented in the dashed rectangle in Fig. 4, was designed for logistical regression and classification rather than regression analysis. All *C. elegans* nematodes were classified into 14 classes, and each class

TABLE 4
THE MEASUREMENT OF *C. ELEGANS* AGE USING THE TESTING ARCHITECTURE SHOWN IN FIG. 4 WITH INCEPTIONV3 AND INCEPTIONRESNETV2, SEPARATELY, WITHOUT CURVED_OR_STRAIGHT

	Validation		Test
	Loss (%)	Accuracy (%)	Accuracy (%)
InceptionV3	1.24	49.05	48.31
InceptionResNetV2	1.17	59.11	57.30

TABLE 5
THE MEASUREMENT OF *C. ELEGANS* AGE USING THE TESTING ARCHITECTURE SHOWN IN FIG. 4 WITH INCEPTIONV3 AND INCEPTIONRESNETV2, SEPARATELY. THE FIRST DENSE LAYER OF THE PROPOSED MODEL SHOWN IN FIG. 4 CONTAINS 64 CELLS FOR CURVED_OR_STRAIGHT

(64 cells for curved_or_straight)	Validation		Test
	Loss (%)	Accuracy (%)	Accuracy (%)
InceptionV3	1.18	49.09	50.00
InceptionResNetV2	0.94	61.21	57.60

presented a specific age from day 1 to day 14. The performance test with the testing architecture shown in Fig. 4 was repeated, and the CNN model separately adopted InceptionV3 and InceptionResNetV2. We present the results without or with curved_or_straight in Table 4 and Table 5, respectively.

As shown in Table 4, without curved_or_straight in the model, InceptionV3 and InceptionResNetV2 achieved accuracies of 48.31% and 57.3%, respectively, in the performance test to measure *C. elegans* age. As shown in Table 5, if curved_or_straight was included in the model, InceptionV3 and InceptionResNetV2 showed small improvements in accuracy, with accuracies of 50% and 57.6%, respectively. The proposed model in Fig. 4 with InceptionResNetV2 outperformed the proposed model with InceptionV3 both with and without curved_or_straight. Upon distributing all measurements of *C. elegans* age in Table 5 on the plot of age prediction, as shown in Fig. 7, we found that the accuracy of the prediction reached 84.78% if the error tolerance was 1 day and 89.13% if the error tolerance was 2 days.

5 DISCUSSION AND CONCLUSION

C. elegans is an important model for studying the regulation of aging and longevity [38]. A method for precisely measuring the physiological age of *C. elegans* would serve as a very useful research tool, especially in large-scale antiaging drug screening or genetic screening studies, where the early and accurate measurement of physiological age would significantly reduce time and resource costs. For example, the effects of various antiaging interventions on the rate of aging could be determined by precisely quantifying

1545-5963 (c) 2019 IEEE. Personal use is permitted, but republication/redistribution requires IEEE permission. See http://www.ieee.org/publications_standards/publications/rights/index.html for more information.
Authorized licensed use limited to: University of Exeter. Downloaded on May 03,2020 at 19:53:28 UTC from IEEE Xplore. Restrictions apply.

This article has been accepted for publication in a future issue of this journal, but has not been fully edited. Content may change prior to final publication. Citation information: DOI 10.1109/TCBB.2020.2971992, IEEE/ACM Transactions on Computational Biology and Bioinformatics

physiological age in the early stage of the aging process (e.g., days 5-9 of adulthood). Based on the experimental results in this paper, we have a complete and robust system for the tool shown in Fig. 8, the architecture of which consists of three main parts: an image normalization module, a database of *C. elegans* images and corresponding attributes, and the CNN model proposed in this paper. The image normalization module shown in Fig. 8 assists in the normalization of the input *C. elegans* image to fit the conditions of the trained CNN model, such as rotation, translation, magnification and illumination. The image normalization module may increase the robustness of the system to various *C. elegans* images. The attributes of *C. elegans* can be manually input or automatically extracted by the image normalization module with traditional image processing methods.

In this paper, we verified that existing CNN models can quantitatively measure *C. elegans* physiological age with good performance. The verified CNN models were VGG16, InceptionV3, InceptionResNetV2, MobileNet, and ResNet50, all of which are successful types of CNN models and have achieved benchmarks in ILSVRC challenges. Moreover, we proposed two CNN models that can satisfy precise, quantitative requirements and achieve a test MAE of less than 1 day and an accuracy close to 90%. These performance values represent great improvements in the measurement of physiological age in *C. elegans* and are of great significance for aging studies. Previously, measurements of the physiological age of *C. elegans* could be differentiated into only certain periods or classes from childhood to elderhood.

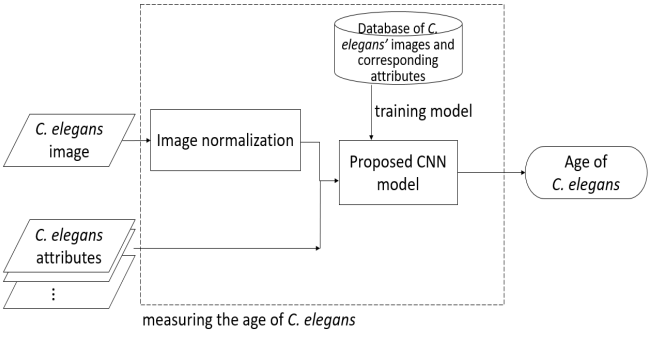

Fig. 8 The components within the dashed rectangle compose the architecture of the complete and robust system for the proposed CNN model.

All selected CNN models discussed in the previous paragraph had achieved good benchmarks in ILSVRC challenges. In the ILSVRC classification task, there were 1,000 object classes, approximately 1.2 million training images, 50,000 validation images and 50,000 test images. However, there were only 913 images in the *C. elegans* image dataset in this paper; this dataset is much smaller than those used in ILSVRC challenges. With the small dataset of *C. elegans* images, the method we proposed achieved an MAE of less than 1 day. Moreover, the images of *C. elegans* used in this paper were photographed with a standard brightfield microscope and not a high-resolution electron microscope. The proposed system could be more cost-efficient and easier to implement than other systems. Therefore, for the training database of *C. elegans* in Fig. 8, we expect that the accuracy of quantitative measurement of *C. elegans* age, using the novel system, might be greatly improved if the training database of *C. elegans* images is enlarged. Before completing the large dataset of *C. elegans* images, transfer learning could be a direction for our next work.

In this paper, in addition to verifying the capabilities of existing CNN models to measure the physiological age of *C. elegans*, we proposed two new models that include the existing CNN model and a feature, curved_or_straight, of *C. elegans*. Adding one feature to assist with the training and recognition of the existing CNN model greatly improved the accuracy of predicting *C. elegans* age. The testing architecture shown in Fig. 2, which used InceptionResNetV2 as the CNN model, achieved a test MAE of 1.18 days. Using the testing architecture illustrated in Fig. 3 and InceptionResNetV2 as the CNN model, the MAE was reduced to 0.94 days, and the accuracy reached 88.92% with an error tolerance of 2 days. We found that the decline in the MAE was approximately 20%. The reason for this great improvement was the involvement of the feature, curved_or_straight. However, an improvement conferred by the attribute curved_or_straight was not attained with all the CNN models, e.g., InceptionV3, as shown in Table 2. Therefore, we expect better results in our next work when using more attributes of *C. elegans*, such as image texture entropy [22] or age-related changes in *C. elegans* (Table 1 in [7]).

TABLE 6
ACCURACY COMPARISON OF THE REGRESSION ANALYSIS AND LOGISTIC REGRESSION MODELS.

	InceptionResNetV2 + 64 cells for curved_or_straight	
	Regression analysis	Logistic regression
Accuracy with 1-day tolerance	55.46%	84.78%
Accuracy with 2-day tolerance	88.92%	89.13%

If the proposed model presented in Fig. 4 with InceptionResNetV2 and 64 cells for the attribute curved_or_straight was used, the accuracy in predicting *C. elegans* age was 57.60%, and the accuracy reached 89.13% with an error tolerance of 2 days. If the proposed model presented in Fig. 3 with InceptionResNetV2 and 64 cells for the attribute curved_or_straight was used, the test MAE of the measurement of *C. elegans* age was 0.94 days. Furthermore, the accuracy reached 89.13% with an error tolerance of 2 days. We found that the accuracy was similar for these two proposed models, as shown in Fig. 3 and Fig. 4. The difference between these two models was that the model in Fig. 3 was designed for regression analysis and outputs a continuous value of age, and the model in Fig. 4 was designed for logistic regression and outputs a discrete value of age. Although the accuracy of the logistic regression model was higher than that of the linear regression model,

1545-5963 (c) 2019 IEEE. Personal use is permitted, but republication/redistribution requires IEEE permission. See http://www.ieee.org/publications_standards/publications/rights/index.html for more information.
Authorized licensed use limited to: University of Exeter. Downloaded on May 03,2020 at 19:53:28 UTC from IEEE Xplore. Restrictions apply.

This article has been accepted for publication in a future issue of this journal, but has not been fully edited. Content may change prior to final publication. Citation information: DOI 10.1109/TCBB.2020.2971992, IEEE/ACM Transactions on Computational Biology and Bioinformatics

as shown in Table 6, we found that the divergence of the distribution of the test results with the logistic regression model, which is shown in Fig. 7, was much higher than that with the regression analysis model, which is shown in Fig. 6. We examined the cases that caused the largest errors in Fig. 7, and the corresponding images are shown in Fig. 9.

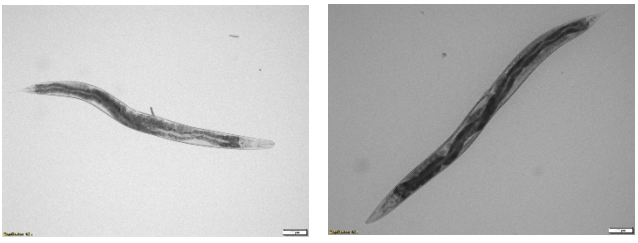

(a) (b)

Fig. 9 (a) The day-2 *C. elegans* that was recognized as day 12, plotted in Fig. 7. (b) The day-12 *C. elegans* that was recognized as day 2, plotted in Fig. 7.

When we visually inspected these two images, based on personal experience, we had difficulty distinguishing them, and might have made the same classification errors as the model. For logistic regression, at the last layer of the proposed model, the activation function adopts the softmax function, which selects the maximum value of all connected cells for the output class. Therefore, these two images may have high, similar values for the classes day 2 and day 12. We are interested in whether the focused features of day 2 and day 12 *C. elegans* in CNN models are highly similar. The focused features in images for the recognition of the CNN model are important issues for our next work.

ACKNOWLEDGMENTS

The following funding source supported this research: the Ministry of Science and Technology of Taiwan (A-L. H.).

REFERENCES

[1] Cen Wan, Alex A. Freitas, and Joao Pedro de Magalhaes, "Predicting the Pro-Longevity or Anti-Longevity Effect of Model Organism Genes with New Hierarchical Feature Selection Methods," *IEEE/ACM Transactions on Computational Biology and Bioinformatics*, 2015 Mar-Apr;12(2):262-75, DOI: 10.1109/TCBB.2014.2355218

[2] Heidi A. Tissenbaum, "Using *C. elegans* for aging research," *Invertebrate Reproduction & Development*, 59:sup1, 59-63, DOI: 10.1080/07924259.2014.940470, 2015

[3] William B. Zhang, Drew B. Sinha, William E. Pittman, Erik Hvatum, Nicholas Stroustrup, and Zachary Pincus, " Extended twilight among isogenic *C. elegans* causes a disproportionate scaling between lifespan and health," *Cell Systems*, 2016 October 26; 3(4): 333–345.e4. DOI:10.1016/j.cels.2016.09.003.

[4] Mark A. Bolanowski, Richard L. Russell and Lewis A. Jacobson, "Quantitative measures of aging in the nematode *Caenorhabditis Elegans*. I. population and longitudinal studies of two behavioral parameters," *Mechanisms of Ageing and Development* 15(3):279–295, 1981, DOI: 10.1016/0047-6374(81)90136-6

[5] Ao-Lin Hsu, Zhaoyang Feng, Meng-Yin Hsieh, and X. Z. Shawn Xu, "Identification by machine vision of the rate of motor activity decline as a lifespan predictor in *C. elegans*," *Neurobiology of Aging*, 2009 September ; 30(9): 1498–1503. DOI:10.1016/j.neurobiolaging.2007.12.007.

[6] Jeong-Hoon Hahm, Sunhee Kim, Race DiLoreto, Cheng Shi, Seung-Jae V. Lee, Coleen T. Murphy & Hong Gil Nam, "*C. elegans* maximum velocity correlates with healthspan and is maintained in worms with an insulin receptor mutation," *Nature Communications*, 2015 November 20; 6:8919. DOI: 10.1038/ncomms9919.

[7] James J. Collins, Cheng Huang, Stacie Hughes and Kerry Kornfeld, "The measurement and analysis of age-related changes in *Caenorhabditis elegans*, " *WormBook*, ed. The *C. elegans* Research Community, WormBook, doi/10.1895/wormbook.1.137.1, http://www.wormbook.org, 2007.

[8] Zhaoyang Feng, Christopher J Cronin, John H Wittig Jr, Paul W Sternberg and William R Schafer, "An imaging system for standardized quantitative analysis of *C. elegans* behavior, " *BMC Bioinformatics*, 5(115):115, 2004 September, DOI: 10.1186/1471-2105-5-115

[9] Christophe Restif and Dimitris Metaxas, "Tracking the swimming motions of *C. elegans* worms with applications in aging studies," *Medical Image Computing and Computer-Assisted Intervention - MICCAI 2008*, 11(Part 1):35-42, DOI: 10.1007/978-3-540-85988-8_5

[10] Josiah Johnston, Wendy B. Iser, David K. Chow, Ilya G. Goldberg, Catherine A. Wolkow, "Quantitative Image Analysis Reveals Distinct Structural Transitions during Aging in *Caenorhabditis elegans* Tissues," PLoS ONE 3(7): e2821, pp:808-814, DOI:10.1371/journal.pone.0002821, 2008

[11] Y. LeCun, B. Boser, J. S. Denker, D. Henderson, R. E. Howard, W. Hubbard, and L. D. Jackel, "Backpropagation applied to handwritten zip code recognition," *Neural Computation*, vol. 1, no. 4, pp. 541–551, Winter 1989.

[12] Alexander Filonenko, Laksono Kurnianggoro, and Kang-Hyun Jo, "Comparative study of modern convolutional neural networks for smoke detection on image data," *International Conference on Human System Interactions*, 2017 July, pp. 64–68, DOI: 10.1109/HSI.2017.8004998.

[13] Olga Russakovsky, Jia Deng, Hao Su, Jonathan Krause, Sanjeev Satheesh, Sean Ma, Zhiheng Huang, Andrej Karpathy, Aditya Khosla, Michael Bernstein, Alexander C. Berg and Li Fei-Fei, "ImageNet Large Scale Visual Recognition Challenge," *International Journal of Computer Vision*, vol. 115, issue 3, pp 211–252, https://doi.org/10.1007/s11263-015-0816-y, 2015.

[14] Eunbyung Park, Wei Liu, Olga Russakovsky, Jia Deng, Fei-Fei Li, and Alex Berg, "Overview of ILSVRC 2017," *Beyond ImageNet Large Scale Visual Recognition Challenge Workshop*, 2017 July 26th.

[15] Neena Aloysius and Geetha M, "A Review on Deep Convolutional Neural Networks," *ICCSP*, April 6-8, 2017, DOI: 10.1109/ICCSP.2017.8286426

[16] Yu Li, Chao Huang, Lizhong Ding, Zhongxiao Li, Yijie Pan, Xin Gao, "Deep learning in bioinformatics: Introduction, application, and perspective in the big data era," *Methods*, 2019 April , vol. 166, pp 4-21, DOI: 10.1016/j.ymeth.2019.04.008

[17] Ramzan Umarov, Hiroyuki Kuwahara, Yu Li, Xin Gao, Victor Solovyev, "Promoter analysis and prediction in the human genome using sequence-based deep learning models," *Bioinfor-*

1545-5963 (c) 2019 IEEE. Personal use is permitted, but republication/redistribution requires IEEE permission. See http://www.ieee.org/publications_standards/publications/rights/index.html for more information.
Authorized licensed use limited to: University of Exeter. Downloaded on May 03,2020 at 19:53:28 UTC from IEEE Xplore. Restrictions apply.

This article has been accepted for publication in a future issue of this journal, but has not been fully edited. Content may change prior to final publication. Citation information: DOI 10.1109/TCBB.2020.2971992, IEEE/ACM Transactions on Computational Biology and Bioinformatics

matics, 35(16), 15 August 2019, pp 2730–2737, DOI: 10.1093/bioinformatics/bty1068

[18] Yu Li, Sheng Wang, Ramzan Umarov, Bingqing Xie, Ming Fan, Lihua Li, Xin Gao, "DEEPre: sequence-based enzyme EC number prediction by deep learning," *Bioinformatics*, 34(5), 2018, pp 760–769, DOI: 10.1093/bioinformatics/btx680

[19] Zhihao Xia, Yu Li , Bin Zhang, Zhongxiao Li, Yuhui Hu, Wei Chen, Xin Gao, "DeeReCT-PolyA: a robust and generic deep learning method for PAS identification," *Bioinformatics*, 35(14), 2019, pp 2371–2379, DOI: 10.1093/bioinformatics/bty991

[20] Ahmad J. Al-Mahasneh, Sreenatha G. Anavatti, and Matthew A. Garratt, "The development of neural networks applications from perceptron to deep learning," *IEEE ICAMIMIA*, 2017 October, DOI: 10.1109/ICAMIMIA.2017.8387619.

[21] Qinhu Zhang, Lin Zhu, Wenzheng Bao, and De-Shuang Huang, "Weakly-Supervised Convolutional Neural Network Architecture for Predicting Protein-DNA Binding," *IEEE/ACM Transactions on Computational Biology and Bioinformatics*, PP(99):1-1, 2018 Aug 7. DOI: 10.1109/TCBB.2018.2864203.

[22] Shuang Cheng, Maozu Guo, Chunyu Wang, Xiaoyan Liu, Yang Liu, and Xuejian Wu, "MiRTDL: A Deep Learning Approach for miRNA Target Prediction," *IEEE/ACM Transactions on Computational Biology and Bioinformatics*, vol. 13, no. 6, pp 1161 – 1169, 22 December 2015, DOI: 10.1109/TCBB.2015.2510002

[23] Cheng Huang, Chengjie Xiong and Kerry Kornfeld, "Measurements of age-related changes of physiological processes that predict lifespan of Caenorhabditis elegans," *Proceedings of the National Academy of Sciences of the United States of America* vol. 101,21 (2004): 8084- 8089, DOI: 10.1073/pnas.0400848101.

[24] Jiunn-Liang Lin, Yung-Sheng Chen, Yi-Hao Huang, Ao-Lin Hsu, Tai-Lang Jong, and Wen-Hsing Hsu, "Approach to the Caenorhabditis elegans segmentation from its microscopic image," *IEEE International Conference on Systems, Man, and Cybernetics*, Oct. 2018, DOI: 10.1109/SMC.2018.00235.

[25] Lior Shamir, Catherine A. Wolkow and Ilya G. Goldberg, " Quantitative measurement of aging using image texture entropy," *Bioinformatics*, vol. 25 no. 23, pp: 3060–3063, 2009 Oct. 6, DOI: 10.1093/bioinformatics/btp571.

[26] Alexander Filonenko, Laksono Kurnianggoro, and Kang-Hyun Jo, "Comparative study of modern convolutional neural networks for smoke detection on image data," *International conference on human system interactions (2017)*, pp. 64–68, DOI: 10.1109/HSI.2017.8004998.

[27] Kaiming He, Xiangyu Zhang, Shaoqing Ren, and Jian Sun, "Deep residual learning for image recognition," *IEEE Conference on Computer Vision and Pattern Recognition (CVPR) 2016*, pp 770–778, arXiv:1512.03385 [cs.CV]

[28] Christian Szegedy, Wei Liu, Yangqing Jia, Pierre Sermanet, Scott Reed, Dragomir Anguelov, Dumitru Erhan, Vincent Vanhoucke, and Andrew Rabinovich, "Going deeper with convolutions," *IEEE Conference on Computer Vision and Pattern Recognition (CVPR), 2015 June*, pp 1–9, DOI: 10.1109/CVPR.2015.7298594.

[29] Sergey Ioffe and Christian Szegedy, "Batch normalization: accelerating deep network training by reducing internal covariate shift," arXiv: 1502.03167 [cs.LG], 2015.

[30] Christian Szegedy, Vincent Vanhoucke, Sergey Ioffe, and Jonathon Shlens, "Rethinking the Inception architecture for computer vision," arXiv: 1512.00567v1 [cs.CV], 2015.

[31] Christian Szegedy, Sergey Ioffe, Vincent Vanhoucke, and Alexander A. Alemi, "Inception-v4, Inception-ResNet and the impact of residual connections on learning," *AAAI Conference on Artificial Intelligence,*" arXiv:1602.07261v2 [cs.CV], 2017

[32] Karen Simonyan and Andrew Zisserman, "Very deep convolutional networks for large-scale image recognition," arXiv: 1409.1556v6 [cs.CV].

[33] Andrew G. Howard, Menglong Zhu, Bo Chen, Dmitry Kalenichenko, Weijun Wang, Tobias Weyand, Marco Andreetto, and Hartwig Adam, "MobileNets: efficient convolutional neural networks for mobile vision applications," arXiv: 1704.04861v1, 2017.

[34] Min Lin, Qiang Chen, Shuicheng Yan, "Network in network," arXiv: 1312.4400. [cs.NE], 2014

[35] Tielin Zhang, Yi Zeng, Bo Xu, "HCNN: A Neural Network Model for Combining Local and Global Features towards Human-like Classification," *International Journal of Pattern Recognition and Artificial Intelligence*, 30(1), 2015 October, DOI: 10.1142/S0218001416550041

[36] Tomoyoshi Shimobaba, Takashi Kakue, and Tomoyoshi Ito , "Convolutional neural network-based regression for depth prediction in digital holography," arXiv:1802.00664 [cs.CV], 2018

[37] Zhicheng Yan, Hao Zhang, Robinson Piramuthu, Vignesh Jagadeesh, Dennis DeCoste, Wei Di, and Yizhou Yu,"HD-CNN: Hierarchical Deep Convolutional Neural Network for Large Scale Visual Recognition," arXiv:1410.0736 [cs.CV], 2015

[38] Tamara R. Golden, Simon Melov, "Gene expression changes associated with aging in *C. elegans*," WormBook, ed. The *C. elegans* Research Community, WormBook, 2007, doi/10.1895/wormbook.1.127.2, http://www.wormbook.org.

Jiunn-Liang Lin received BEng and MEng degrees in electrical engineering from National Tsing Hua University in 1987 and 1989, respectively. He has worked for the Industrial Technology Research Institute since 1991. He has been working toward a PhD degree in the Department of Electrical Engineering, National Tsing Hua University, since 2010. His research interests include image processing and neural networks.

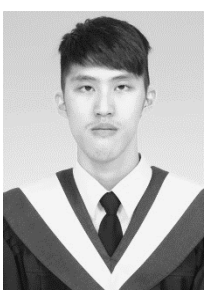

Wei-Liang Kuo received a BS degree in communications from National Central University, Taiwan, in 2015 and an MS degree in electrical engineering from National Tsing Hua University (NTHU), Taiwan, in 2018. His research interests include machine learning and deep learning. After graduating from NTHU, he has worked at MediaTek for half a year.

Yi-Hao Huang received a BS degree in biological science and technology and an MS degree in cancer biology from China Medical University, Taiwan, in 2013 and 2015, respectively. He currently is pursuing a PhD degree in Ao-Lin Hsu's laboratory at the Institute of Biochemistry and Molecular Biology, National Yang-Ming University, Taiwan. His research interests include aging biology and neuroscience.

1545-5963 (c) 2019 IEEE. Personal use is permitted, but republication/redistribution requires IEEE permission. See http://www.ieee.org/publications_standards/publications/rights/index.html for more information.
Authorized licensed use limited to: University of Exeter. Downloaded on May 03,2020 at 19:53:28 UTC from IEEE Xplore. Restrictions apply.

This article has been accepted for publication in a future issue of this journal, but has not been fully edited. Content may change prior to final publication. Citation information: DOI 10.1109/TCBB.2020.2971992, IEEE/ACM Transactions on Computational Biology and Bioinformatics

Tai-Lang Jong received BSEE and MSEE degrees from National Tsing Hua University and a PhD from Texas Tech University, Lubbock, in 1990. Since 1990, he has been with the Department of Electrical Engineering, National Tsing Hua University, Hsinchu, Taiwan (R.O.C.), where he is currently an Associate Professor. He is currently responsible for managing the DSP teaching laboratory for the department. He also serves as one of the committee members on the university's Computer and Communications Committee.

Ao-Lin Hsu received a BS degree in chemistry from National Taiwan University and a PhD degree in medicinal chemistry from the University of Kentucky, College of Pharmacy, in December 2000. After postdoctoral studies in Biochemistry and Biophysics at UC San Francisco, he then joined the faculty of the University of Michigan in 2004 as an Assistant Professor. His laboratory works on the molecular genetics of aging using *C. elegans* as a model organism. Dr. Hsu is a recipient of the New Scholar Award in Aging (2005-2009) from the Ellison Medical Foundation. He is currently a professor at the Institute of Biochemistry and Molecular Biology at the National Yang-Ming University, Taiwan.

Wen-Hsing Hsu received a BS degree in electrical engineering from National Cheng Kung University, Taiwan, in 1972, and ME and PhD degrees in electrical engineering from Keio University, Japan, in 1978 and 1982, respectively. In 1982, he joined the Department of Electrical Engineering, National Tsing Hua University, Taiwan, where he is now a professor. His research interests include image processing, biologic identification, and network security. Dr. Hsu is a member of the Institute of Electronics, Information and Communication Engineers (IEICE), the Information Processing Society of Japan, and the Chinese Association of Image Processing and Pattern Recognition.

1545-5963 (c) 2019 IEEE. Personal use is permitted, but republication/redistribution requires IEEE permission. See http://www.ieee.org/publications_standards/publications/rights/index.html for more information.
Authorized licensed use limited to: University of Exeter. Downloaded on May 03,2020 at 19:53:28 UTC from IEEE Xplore. Restrictions apply.